Simulation Study of GPS Phase Scintillation

Charles L. Rino (1),(2), Charles Carrano (1), Joy Jao (2), Brian Breitsch (2), and Jade Morton (2)
(1) Boston College, Institute for Scientific Research, Chestnut Hill, MA
(2) Colorado State University, Department of Electrical and Computer Engineering, Fort Collins, CO

Version: May 1, 2017

Signal phase measured by GPS signal processors is crucial for high-resolution range measurement. However, the measured signal phase must be corrected for the the dispersive phase advance imposed by the earth's ionosphere. Dual-frequency measurements exploit frequency dependence to isolate and correct the ionosphere-induced phase change. The correction is proportional to total electron content (TEC), which can be used as an ionospheric diagnostic in its own right.

New theoretical results have provided a means of efficiently generating multi-frequency scintillation realizations over the complete range of observed GPS disturbance levels. A compact parameterization allows space-to-time translation consistent with observed temporal variations. Moreover, the stochastic TEC variation that initiates the phase-screen realization is effectively TEC truth, whereby scintillation-induced TEC errors can be evaluated.

TEC truth also provides a means of assessing the relation between deep fades and associated rapid phase changes that are often identified as *cycle slips*. We assess the conditions under which scintillation imposes irrecoverable TEC errors. Because the simulations are free of scintillation-induced processor distortions, the errors are effectively lower bounds.

Key Words: GPS, Scintillation, Modeling, Numerical Simulation

1. INTRODUCTION

GPS receivers measure signal intensity, I, phase, ϕ, and delay, τ. In the absence of multipath, clock errors, biases, and noise, the following ideal relations characterize the measurements:

$$I\left(t;f_c\right) = P(t)\left|h\left(t;f_c\right)\right|^2 \tag{1}$$

$$\left(c/(2\pi f_c)\right)\phi\left(t;f_c\right) = r\left(t\right) + cKN\left(t\right)/\left(2\pi f_c^2\right) + c\phi_s\left(t;f_c\right)/\left(2\pi f_c\right) + M\lambda_c \tag{2}$$

$$c\tau\left(t;f_c\right) = r\left(t\right) - cKN\left(t\right)/\left(2\pi f_c^2\right) - c\phi_s\left(t;f_c\right)/\left(2\pi f_c\right). \tag{3}$$

The defining parameters represent range, $r\left(t\right)$, frequency, f_c, the velocity of light, c, TEC to phase conversion, $K = 1.3454 \times 10^9\ m^2/s$ ($\phi = 2\pi KN/f_c$), and path-integrated TEC, $N\left(t\right)$. Delay and phase have been scaled to have common range units. The term $M\lambda_c$, where $\lambda_c = c/f_c$ represents wavelength, is the phase ambiguity. The term $P(t)$ accommodates signal intensity variation other than scintillation. Scintillation is characterized by the complex modulation

$$h\left(t;f_c\right) = \left|h\left(t;f_c\right)\right|\exp\{i\phi_s\left(t;f_c\right)\}. \tag{4}$$

Differencing the pseudo range delay and the phase advance in delay units determines M. Dual-frequency phase measurements can be used to isolate the TEC contribution:

$$TEC_k \simeq \frac{\phi_k^{[2]}/f_{c_2} - \phi_k^{[1]}/f_{c_1}}{2\pi K\left(1/f_{c_2}^2 - 1/f_{c_2}^2\right)}, \tag{5}$$

where the k index represent sample number and the two frequencies are designated 1 and 2. However, we note that although separate TEC and scintillation contributions to the signal phase have been introduced explicitly, the only observable distinction comes from the frequency dependence. That is, to the extent that $\phi_s\left(t; f_c\right) \propto 1/f_c$ the signal phase component will be isolated and corrected as *stochastic* TEC.

In the remainder of this paper (5) will be taken as a defining relation, with $\phi_s\left(t; f_c\right)$ generated with a two-dimensional phase screen realizations. The initiating stochastic phase realization is TEC truth. As the field at the phase screen propagates to the observation plane, diffraction generates intensity scintillation and modification of the initiating path-integrated phase. The phase-screen theory is described in Carrano and Rino [1].

2. PHASE-SCREEN REALIZATIONS

In the phase-screen theory the initiating stochastic path-integrated phase structure is characterized by the normalized one-dimensional phase spectral density function (SDF)

$$P\left(\mu\right) = \left(C_p \rho_F^{p_1 - 1}\right) \begin{cases} \mu^{-p_1} & \text{for } \mu_0 \geqq 1 \\ \mu_0^{p_2 - p_1} \mu^{-p_2} & \text{for } \mu_0 < 1 \end{cases}. \tag{6}$$

where, $\mu = q\rho_F$, $\mu_0 = q_0\rho_F$, and

$$\rho_F = \sqrt{x/k} \tag{7}$$

is the Fresnel scale. A realization of path-integrated phase is generated as follows

$$\overline{\phi}_k = \sum_{n=0}^{N-1} \sqrt{P\left(n\Delta\mu\right)\Delta\mu/\left(2\pi\right)}\eta_n \exp\{-2\pi i n k/N\}, \tag{8}$$

where η_n is a zero-mean, unity-variance, uncorrelated complex random process with the Hermitian property $\eta_n^* = \eta_{N-n}$. A realization of the complex random field at the distance corresponding to to ρ_F is constructed with the following forward and inverse discrete Fourier transformations:

$$\widehat{h}(0; n\Delta\mu) = \sum_{k=0}^{N-1} \exp\{i\overline{\phi}_k\} \exp\left\{-2\pi i n k/N\right\} \tag{9}$$

$$h_k = \frac{1}{N} \sum_{n=0}^{N-1} \widehat{h}(0; n\Delta\mu) \exp\left\{-i\left(n\Delta\mu\right)^2/2\right\} \exp\left\{2\pi i n k/N\right\} \tag{10}$$

Note that neither the frequency nor the Fresnel scale enter (9) and (10) explicitly. The potential scintillation structure, including $S4$ is completely defined by the scale-free parameters. The dependence on the Fresnel scale depends determines how far from the phase screen the structure simposed by the phase screen is observed.

Space-to-time conversion imposes an effective scan velocity, $v_{\rm eff}$, such that $y = v_{\rm eff}t$. The conversion from the Doppler frequency, f_D, to normalized spatial wavenumber follows as

$$\mu = 2\pi f_D \left(\rho_F / v_{\rm eff}\right). \tag{11}$$

To summarize, a phase-screen scintillation surrogate is completely specified by the normalized structure parameters $C_{pp} = C_p \rho_F^{p_1 - 1}$, p_1, p_2, μ_0, the ratio $\rho_F / v_{\rm eff}$, the sample interval Δt, and the number of samples N. By using a common seed to generate η_n with frequency-dependent parameters appropriately scaled, consistent multi-frequency surrogates are realized. Phase-screen theory determines parameter values that will achieve different disturbance levels. Using a highly efficient implementation of the theory developed by Carrano, the intensity SDF, $I(\mu)$, can be evaluated as a function of p_1, p_2, μ_0, and the universal strength parameter

$$U = \left(C_p \rho_F^{p_1 - 1}\right) \begin{cases} 1 & \text{for } \mu_0 \geqq 1 \\ \mu_0^{p_2 - p_1} & \text{for } \mu_0 < 1 \end{cases}. \tag{12}$$

The universal strength parameter orders the scintillation strength such that $U < 1$ corresponds to weak to moderate scatter. $U > 1$ corresponds to strong scatter with $S4$ approaching or exceeding unity.

3. EXAMPLES

Figures 1, 2, and 3 summarize three simulations with perturbation strength increasing from weak to strong. The left-hand frames show the L1, L2, and L5 intensity over a 3-min interval. The defining L1 phase-screen parameters are summarized in the figure titles. The power-law index parameters were set at $p_1 = p_2 = 3$ for $U < 1$, and $p_1 = 2.5$, $q_0 = 2\pi/1000$, $p_2 = 3.5$ for $U \geq 1$ as representative values. Slant TEC estimates derived from (5) using the L1-L2 (red) and L1-L5 (blue) reconstructed phase realizations are overlaid in the upper right-hand frames of each figure. The magenta curve is the initiating phase screen realization converted to TEC units. The middle frame in each segment is the difference between the L12 and L25 TEC estimates, which is a measure that can be derived from real signal phase data. Either way, no detrending is applied to the signal phase prior to generating TEC estimates. The lower right-hand frame in each figure is the probability density function of $\Delta STEC$. We note first that good agreement between the L12 and L15 TEC estimates does not imply an equivalent level of agreement between either estimator and the initiating phase-screen. To the extent that there is measurable intensity scintillation there is accompanying phase scintillation. For weak to moderate perturbation levels ($U < 0.5$), the TEC errors are generally neglibible. In the intensity summaries scintillation fades that exceed -20 dB are marked. As a working definition, if there are no L2 or L5 fades greater than -20 dB, TEC errors are neglibible. As U approaches one, large discreet TEC errors occur. The errors are invariably associated with a fade in excess of -20 dB on one of the contributing frequencies.

4. DISCUSSION

Beyond scintillation-induced TEC errors, the phase-screen model provides insight into scintillation characterization. From well-sampled simulations continuous phase can be recovered through any fade. Thus, strickly speaking, there are no

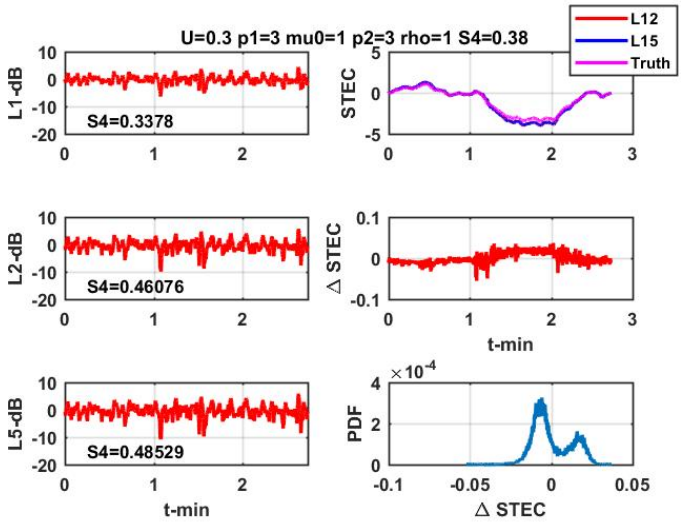

FIG. 1 Weak disturbance.

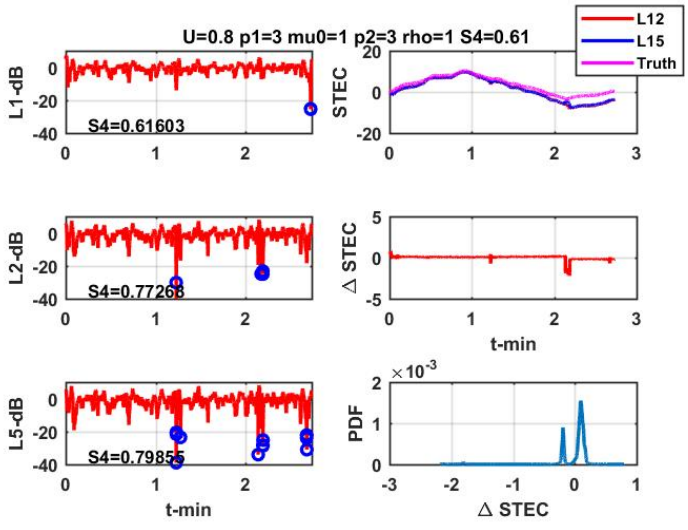

FIG. 2 Moderate disturbance.

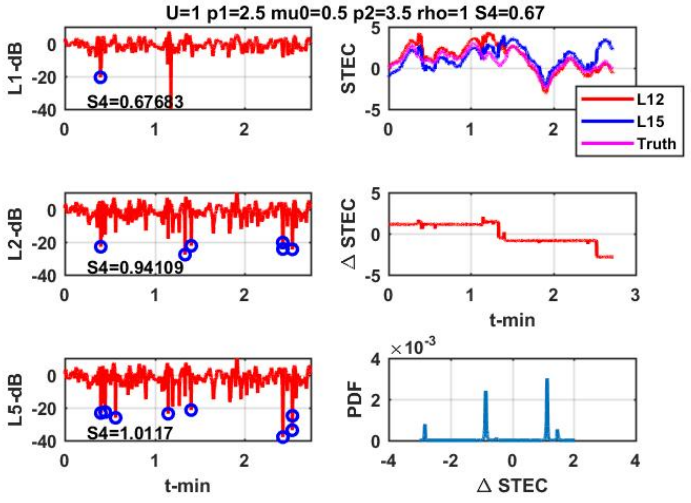

FIG. 3 Strong disturbance.

single-frequency phase discontinuities. However, phase changes approaching 100 radians per second were observed within a continuous phase variation range of several hundred radians. Step STEC changes are caused by departures from the dispersive phase frequency variation. The changes are generally associated with but not necessarily concident with a deep fade on one of the contributing frequencies.

The phase-screen theory provides a basis for interpretive parameter estimation, which attempts to find a best-fit between measured intensity SDFs and theoretical predictions, as described in Carrano and Rino [1]. The phase-screen model uses the ideal realization as a surrogate. Figure 4 shows the strong disturbance L1 phase and intensity SDFs with the theoretical initiating phase and intensity SDFs overlaid. Whereas we expect the theory to agree very well with the measured intensity SDF, the fact that the initiating phase also agrees with the measured phase SDF is an observation. Although there is no theory that predicts phase structure measures, the initiating phase SDF is a good guidline. The structure as driven by C_{pp} can be scaled so that the intensity scintillation is below the noise while phase structure remains. Such intensity-scintillation-free data are ideally suited for GPS operations. Under such conditions measures that capture the stochastic TEC structure are the appropriate extensions of the theory. The key is separating the geographic range contribution from the TEC. This cannot be done perfectly with a single-frequency measurement, but C_{pp} and p_1 can be estimated from appropriately detrended signal phase measurements. From the theory, the largest ρ_F value that places intensity scintillation at the noise level is a bound.

REFERENCES

[1] C. S. Carrano and C. L. Rino. A theory of scintillation for two-component power law irregularity spectra: Overview and numerical results. *Radio Sci.*, 51(doi:10.1002/2015RS005903):789âĂŞ813, 2016.

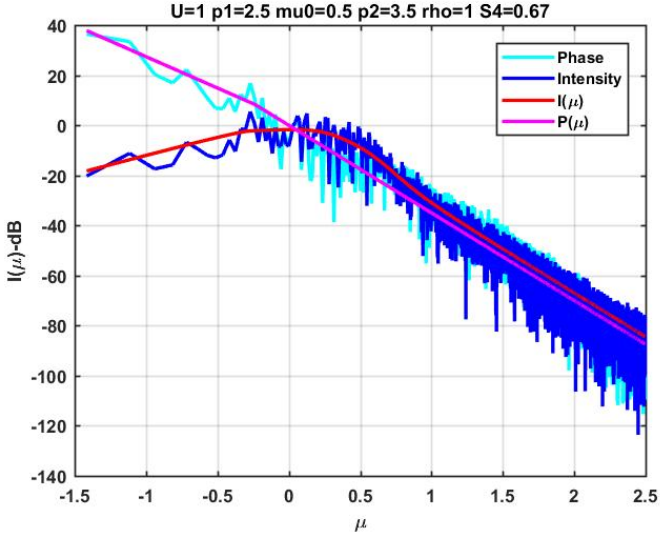

FIG. 4 Theory and measured surrogate SDF comparisons.